Integrating Satellite Images Segmentation and Electrical Infrastructure Data to Identify Possible Urban Irregularities in Power Grid

Álisson Alves[1,2][a], Luísa Souza[1,2][b], Luiz Cho-Luck[1][c], Raniere Lima[1][d], Carlos Augusto[1][e], Wesley Marinho[1,2][f], Rafael Capuano[1][g], Bruno Costa[1][h], Marina Siqueira[1][i], Jesaías Silva[1][j], Raul Paradeda[3][k] and Pablo Javier Alsina[2][l]

[1]*SENAI Institute of Innovation in Renewable Energy, Capitão-Mor Gouveia Avenue, Natal-RN, Brazil*

[2]*Graduate Program in Electrical and Computer Engineering, Federal University of Rio Grande do Norte, Natal-RN, Brazil*

[3]*Department of Computer Science, State University of Rio Grande do Norte, Dr. João Medeiros Filho Avenue, Natal-RN, Brazil*

Abstract: Managing urban expansion and its impact on electrical infrastructure presents significant challenges, necessitating innovative methodologies to address irregular settlements and commercial losses in the electricity sector. This paper proposes an approach integrating convolutional neural networks and geospatial data to detect urban areas lacking electrical infrastructure. High-resolution Google Earth images and low-resolution Landsat 8 data were processed using advanced semantic segmentation architectures, LinkNetB7 and D-LinkNet50, to analyze land use patterns. The segmentation outputs were combined with data from the Brazilian Geographic Database of the Distribution System to generate comprehensive maps of electrical infrastructure coverage. The study focused on the SBAU substation in Sabará, Minas Gerais, which demonstrated commercial losses of up to 47.5% in specific feeders. Results demonstrated the effectiveness of deep learning models in identifying mismatches between urban development and infrastructure coverage, highlighting areas with potential irregular connections. This study contributes to advancing artificial intelligence applications in urban energy management by providing a scalable framework for analyzing land use and electrical infrastructure.

1 INTRODUCTION

In Brazil, electricity consumption increased by 12.6% between 2014 and 2023, reaching an all-time high of 616.3 TWh in 2023, according to the Brazilian Energy Research Company (EPE, 2024). The industrial (36.4%) and residential (27.5%) sectors dominate the country's energy consumption profile, particularly in the Southeast, which accounts for nearly half of the national demand (EPE, 2024; Flores et al., 2023). This rising demand underscores the importance of efficient infrastructure planning in densely populated regions. Additionally, sectors such as livestock, though accounting for only 5% of total electricity consumption, significantly influence land use and land cover changes (LULC) (Flores et al., 2023, p. 22).

Understanding LULC changes is critical for addressing the impacts of urbanization on electrical infrastructure. Advances in remote sensing and deep learning have proven instrumental in this domain, particularly in the segmentation of satellite images to map urban and peri-urban areas (Archana and Jeevaraj, 2024; Abujayyab et al., 2023). Convolutional neural network (CNN) architectures excel at processing multi-resolution geospatial data, enabling the detection of urban patterns with high precision, even

[a] https://orcid.org/0000-0002-7999-8189
[b] https://orcid.org/0000-0002-3707-2097
[c] https://orcid.org/0009-0003-7053-0453
[d] https://orcid.org/0009-0006-2677-2983
[e] https://orcid.org/0009-0000-7708-348X
[f] https://orcid.org/0009-0009-7101-1632
[g] https://orcid.org/0009-0004-9627-8177
[h] https://orcid.org/0009-0003-7980-7332
[i] https://orcid.org/0009-0005-2446-8753
[j] https://orcid.org/0000-0002-6586-8340
[k] https://orcid.org/0000-0002-4031-6275
[l] https://orcid.org/0000-0002-2882-5237

under challenging conditions of spatial and temporal variation (Ataş, 2023).

This study builds on these advances by integrating remote sensing data with georeferenced electrical infrastructure datasets, specifically the Brazilian Geographic Database of the Distribution System (BGDDS). By leveraging high-resolution Google Earth imagery and low-resolution Landsat 8 data, combined with advanced CNN-based segmentation architectures, this work identifies discrepancies between urban land use and electrical infrastructure coverage. These insights aim to support urban energy planning and mitigate commercial losses in Brazil's electricity sector.

2 RELATED WORKS

This section presents the main related works that utilize machine learning and deep learning approaches to evaluate land use and land cover in urban contexts, highlighting their advances, challenges, and contributions in processing and analyzing remote sensing data.

Khan and Sudheer (2022) applied a combination of Artificial Neural Networks and Cellular Automata (ANN-CA) to model urban growth in Islamabad, Pakistan, and project future land use changes. The study utilized Landsat image data from 1991 to 2021 to assess the increase in urbanized areas and predict their future expansion by 2041. The approach highlighted the unplanned growth of the city, emphasizing the importance of policy interventions to mitigate negative environmental impacts, such as the loss of green spaces.

The extraction of LULC class features was also addressed by Rani et al. (2024), who utilized the U-Net model to perform semantic segmentation of satellite images. The study demonstrated the effectiveness of U-Net for extracting features of buildings, vegetation, and water bodies from high-resolution images, achieving an F1 score of 92%. The application of this automated technique enables rapid classification of large datasets, reducing the need for human intervention and enhancing the efficiency of land use analysis.

The study by He et al. (2024) focused on the detailed classification of urban buildings using a deep neural network for low-resolution satellite images. The research proposed UB-FineNet, a model that addresses the class imbalance problem by applying high-resolution techniques and contrastive learning. This approach provides a robust solution for fine-grained building classification in large urban areas,

supporting urban planning and resource management.

Ullah et al. (2024) investigated the impact of land use changes on land surface temperature (LST) in Kabul, Afghanistan. Using a combination of support vector machines (SVM) and cellular automata with logistic regression (CA-LR), the study demonstrated a direct correlation between urbanization and rising air temperatures. Projections for 2046 indicate an increase in urbanized areas and, consequently, higher surface temperatures, highlighting the adverse effects of unplanned urban expansion on the local atmosphere.

Although numerous studies apply machine learning techniques for LULC prediction, urban detection, and environmental impact analysis, little research explores the relationship between unplanned urban development and its impact on electrical infrastructure. Issues such as illegal connections and irregular settlements, exacerbated by deeply rooted cultural practices, compromise the efficiency, safety, and planning of the electrical system. In this context, the use of machine learning to identify urbanized areas, analyze energy demands and predict potential anomalies in consumption within these regions can offer valuable solutions for sustainable urban planning.

3 METHODOLOGY

The methodology employs deep learning techniques to analyze urban growth through satellite image segmentation, identifying land use and land cover areas. The process involved acquiring and preprocessing images and binary masks, training segmentation algorithms with labeled data, and analyzing urban density based on the BGDDS. Additionally, an energy balance framework was used to evaluate non-technical losses (NTL) by region and detect anomalies in feeder measurements.

3.1 Datasets Used

3.1.1 Satellite Sensors and Image Preprocessing

To examine the impact of different resolution levels on land use segmentation, images of varying resolutions were obtained. A Python script automated the download of high-resolution Google Earth images (50-60 cm/pixel) and low-resolution Landsat 8 images (30 m/pixel), using binary masks from Open Buildings V3 Polygons (Sirko et al., 2021) and the MapBiomas project (Rosa et al., 2019). Preprocessing involved converting images to PNG, segmenting them into 384 × 384 pixel patches, and balancing the

dataset to remove pairs without pixels of interest.

Google Earth, via Google Earth Engine (Gorelick, 2013), provided high-resolution images from urban areas of Brazil. Thirty images (8192 × 3059 pixels) were processed using a cropping algorithm, generating approximately 5040 smaller images. A filter removed pairs without white pixels (buildings), leaving 1029 balanced pairs. Figure 1 illustrates an example of an image and its corresponding binary mask, obtained from Open Buildings V3 Polygons, which details building outlines.
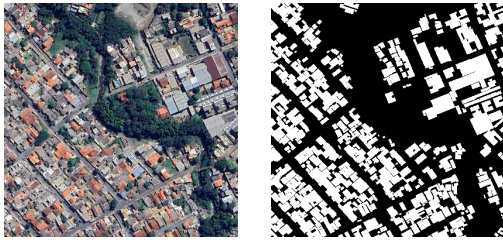
(a) Google Earth image.   (b) Open Buildings mask.

Figure 1: Pair of Google Earth images of a region of Brazil containing a cut-out of a satellite image in its original composition (RGB) with its respective mask obtained through the Open Buildings V3 Polygons.

The **Landsat 8** satellite (Avdan and Jovanovska, 2016) has two main sensors: OLI (Operational Land Imager) and TIRS (Thermal Infrared Sensor). The OLI captures multispectral images in nine bands with a 30-meter spatial resolution, while the TIRS collects data in two thermal bands with a 100-meter resolution, resampled to 30 meters to align with the OLI. For this study, 30-meter multispectral images were used, with a temporal resolution of 16 days and 510 images in total. The Figure 2 shows an example of an RGB image and the reference mask.

(a) Landsat 8 image.   (b) MapBiomas mask.

Figure 2: Pair of images with 30 meters per pixel resolution for neural network training. (a) RGB satellite image from Landsat 8. (b) Groundtruth of land cover from MapBiomas.

3.1.2 Brazilian Geographic Database of the Distribution System

The Brazilian National Electric Energy Agency (ANEEL) mandates electricity distributors to provide BGDDS, an annually updated geographic model that represents Brazil's electrical system, detailing assets such as operational areas and infrastructure, including high, medium, and low voltage networks, transformers, poles, feeders, substations, and transmission towers. BGDDS supports grid planning, operation, and oversight, ensuring infrastructure keeps pace with urban growth. In this study, this data was used to map the electrical infrastructure of Minas Gerais, integrating remote sensing to identify built-up areas lacking network coverage.

3.1.3 Integrated Framework for Monitoring the Distribution Electrical Grid

Given the extensive number of assets managed by a Brazilian electrical company, a tool was developed to ensure energy balance consistency and assess commercial losses at different levels (feeder, substation, and region). The **Framework** integrates data from operational measurements, telemetry-based loss assessments, load flow analysis, and BGDDS network information with monthly energy load records.

The validation process begins with data extraction from the Framework database, followed by an ETL (Extract, Transform, Load) workflow. Data is preprocessed to remove inconsistencies, handle missing values, and align with company standards. Once validated, the dataset is formatted into a JSON payload for advanced analysis.

This approach enables ranking substations by annual commercial losses, identifying problematic feeders, and calculating expected consumption based on measured data, technical losses, and distributed generation, simulating ideal conditions without commercial losses.

3.2 Image Segmentation Algorithms: Architectures and Basic Characteristics

Semantic segmentation is a crucial technique in computer vision that classifies each pixel in an image into categories such as roads, buildings, vegetation, and water. In this context, CNN-based models have demonstrated superior precision and computational efficiency compared to traditional methods (Jiwani et al., 2021). For this study, two semantic segmentation algorithms were applied to divide an image into semantically meaningful regions, labeling each pixel according to its respective class. The architectures used for the analysis of various remote sensors were LinkNetB7 and D-LinkNet50, they will be described next.

3.2.1 Convolutional Neural Networks Architectures

The first semantic segmentation neural network used was LinkNetB7 (Chaurasia and Culurciello, 2017), which employs a pretrained EfficientNet-B7 as its encoder, enhancing feature extraction and model generalization. With compound scaling for parameter adjustment (Akyel and Arıcı, 2022), the architecture combines encoder blocks (dimensionality reduction) and decoder blocks (image reconstruction), using batch normalization, ReLU, skip connections, and class weighting to improve segmentation. Simple and efficient, the model requires less data and training time while maintaining results comparable to other methodologies (Figure 10 B).

The second neural network used was D-LinkNet50 (Zhou et al., 2018), originally designed for road segmentation in satellite images but adaptable to other domains with parameter and label adjustments. It employs ResNet50 as its encoder, a 50-layer network suitable for complex tasks (Li and Liu, 2022). Its architecture, illustrated in Figure 10 (A), is divided into three blocks: A (encoder, which generates a compact latent representation), B (uses dilated convolutions to expand the receptive field while preserving spatial details), and C (decoder, which restores image resolution via transposed convolutions, similar to LinkNet) Zhou et al. (2018).

3.2.2 Training Parameters and Environment

The training hyperparameters were defined based on the literature (Zhou et al., 2018; Akyel and Arıcı, 2022) and previous experiments, including an initial learning rate of 0.001, a binarization threshold of 0.3, and a batch size of 8. Two loss functions were tested: BCE IoU, which combines Binary Cross Entropy and IoU to penalize discrepancies and overlaps (Batchkala and Ali, 2021), and Dice BCE, which balances local and global accuracy in segmentation (Montazerolghaem et al., 2023). To avoid overfitting (Afaq and Rao, 2020), training was limited to 60 epochs with early stopping after five epochs without significant improvement in the loss curve.

Data augmentation techniques, such as rotation, flipping, and shifting, were applied, generating 12 variations per training image to improve model generalization. Non-augmented satellite images were used for validation, ensuring artificial diversification and robust learning. The algorithms were implemented in Python using PyTorch, running on a machine with an AMD Ryzen Threadripper 3970X x64 processor and an NVIDIA GeForce RTX 4090 GPU (24 GB),

accelerated by the CUDA toolkit, complemented by 256 GB of RAM.

3.3 Detection of Urban Areas Covered by Electrical Infrastructure

The methodology is based on the principle that areas with high urban occupation but lacking electrical infrastructure are susceptible to irregular settlements and illegal connections. To identify them, a map of the electrical infrastructure was created using the 'PONNOT' layer from BGDDS, filtering only poles in urban areas, which represent the highest capillarity of the grid (Figure 4). Image segmentation identified occupied areas not covered by the map, generating insights into regions prone to illegal connections. This information enables operational teams to act more assertively in combating commercial losses.

The PONNOT buffer, which simulates the coverage of electrical infrastructure from poles, was created using mathematical morphology techniques. The closing operation, composed of dilation (boundary expansion) and erosion (boundary refinement) with the same structuring element (SE), was applied to smooth contours, fill gaps, and connect nearby areas, ensuring continuous coverage (Gonzalez and Woods, 2000; Solomon and Breckon, 2013). This approach eliminated gaps between buffers, resulting in a homogeneous area (Figure 4). The final electrical infrastructure coverage map is presented in Section 4.

4 RESULTS AND DISCUSSIONS

The study area was selected based on two criteria: urbanization and supply by a substation with high commercial losses. The SBAU substation, located in Sabará, Minas Gerais, met these criteria, recording a commercial loss of 32.094 MWh in 2023, equivalent to 26% of all measured energy—well above the national average of 6.7% (ANEEL, 2025).

SBAU serves $\sim 30,000$ low and medium-voltage customers across ~ 85 km^2 through four feeders: SBAU02, SBAU03, SBAU04, and SBAU05. Figure 5 shows their historical measurement data. SBAU05 (Figure 5 d) had the highest commercial loss rate (47.5%), aligning with studies linking non-technical losses to socioeconomic factors (ANEEL, 2025). Notably, its data consistency suggests it as a key case for loss mitigation studies.

Other feeders also exhibit relevant patterns. SBAU02 (Figure 5 a) had the lowest loss (6%) in 2023, serving the fewest customers. SBAU03 (Figure 5 b) showed stable losses with three notable vari-
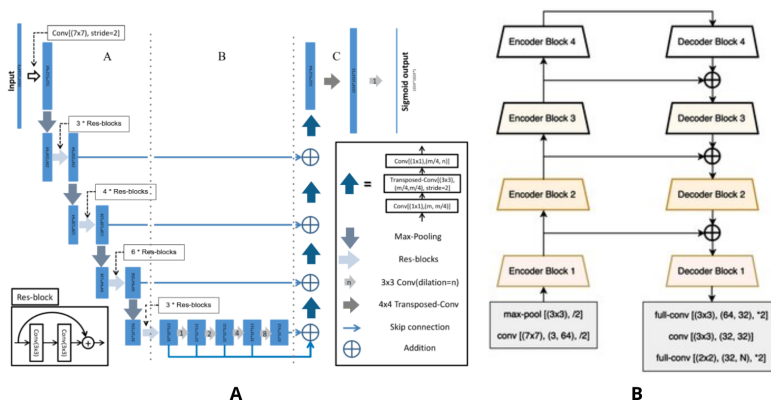
Figure 3: (a) Architecture of the D-LinkNet50 Deep Neural Network, (B) LinkNet Deep Neural Network Architecture. Adapted from: Chaurasia and Culurciello (2017); Zhou et al. (2018).

Figure 4: The image illustrates the PONNOT points (yellow) representing electrical infrastructure poles and their corresponding buffers (green), which simulate the coverage area of electrical infrastructure.

ations, while SBAU04 (Figure 5 c) had pronounced fluctuations, possibly due to operational maneuvers or irregularities.

Following this analysis, the next step was to assess the pole infrastructure coverage in the feeder-supplied regions to identify buildings not connected to the energy grid.

After training and validating the satellite image segmentation models for land use and land cover detection, performance metrics such as accuracy, f1-score, and IoU were evaluated. Additionally, Table 1 presents the number of epochs required for each model to reach the stopping criterion, as well as the corresponding training time.

Deep learning techniques, such as U-Net, achieve up to 95% accuracy in land use classification (Ágton de Oliveira, 2020). However, the choice of architecture and loss function depends on image resolution and application context. High-resolution images are ideal for detailed building identification, whereas lower-resolution images are better suited for large-scale detection tasks.

For Google Earth images, BCEIoU loss yielded the best performance for LinkNetB7, reaching optimal results in 30 epochs. In contrast, DICE BCE achieved the highest overall accuracy, requiring 36 epochs and a training time of 4 hours and 38 minutes. For Landsat 8, LinkNetB7 combined with DICE BCE achieved an impressive accuracy of 0.97 in just 12 epochs.

Table 1 highlights the significant impact of architecture and loss function on segmentation performance. BCE IoU proved superior for high-resolution images, while DICE BCE outperformed in lower-resolution scenarios. The variation in training time and required epochs underscores the importance of careful model selection based on the specific task and data characteristics.

Figures 6 and 8 provide qualitative insights into the model's performance, showcasing its ability to handle both detailed and large-scale features. Additionally, Figures 7 and 9 present the prediction masks for Google Earth and Landsat 8 images, respectively, further illustrating the model's adaptability across different resolutions.

Google Earth images enable individual building block differentiation, whereas Landsat 8 images reveal only occupation patches. High-resolution images are preferred for precise urban monitoring, as they differentiate individual lots, crucial for detailed analysis. In contrast, low-resolution images merge multiple lots, reducing clarity but remaining useful for tracking rapid urban growth. Sensor selection should align with monitoring needs: low-resolution images suit dense or rapidly urbanizing areas, where changes are more noticeable at the edges, while high-resolution images are essential for low-density regions, such as rural areas, to detect subtle land use changes.

Figure 10 (A and B) present maps generated through semantic segmentation of land use and oc-

(a) SBA02

(b) SBA03

(c) SBA04

(d) SBA05

Figure 5: Historical series of feeder measurements, expected consumption, and NTL for the SBAU substation.

Table 1: Performance of the Segmentation Neural Network trained with images from different sensors.

Satellite Sensor	Architecture	Loss Function	Accuracy	F1-Score	IoU	Epochs	Training Time
Google Earth (∼ 0,60 m / pixel)	LinkNetB7	BCEIoU	0,86	0,78	0,77	30	10 h 19 min
	LinkNetB7	DICE BCE	0,85	0,77	0,76	6	2 h 19 min
	D-LinkNet50	BCEIoU	0,84	0,75	0,74	28	9 h 22 min
	D-LinkNet50	DICE BCE	0,84	0,75	0,73	27	9 h 01 min
Landsat 8 (30 m / pixel)	LinkNetB7	BCEIoU	0,96	0,96	0,93	46	7 h 26 min
	LinkNetB7	DICE BCE	0,97	0,96	0,94	12	2 h 03 min
	D-LinkNet50	BCEIoU	0,94	0,92	0,88	19	3 h 04 min
	D-LinkNet50	DICE BCE	0,95	0,94	0,90	16	2 h 36 min

(a)   (b)   (c)   (d)   (e)

Figure 6: Prediction results overlaid on the original for the Google Earth satellite image. (a) Original image; (b) LinkNetB7 BCEIoU; (c) LinkNetB7 DICE BCE; (d) D-LinkNet50 BCEIoU; (e) D-LinkNet50 DICE BCE.

cupation, overlaid with electrical infrastructure coverage (in green). Urban areas are highlighted (in red), emphasizing densely occupied regions, particularly those without electrical grid access.

As shown in Figure 10 (A and B), regions near the SBAU05 and SBAU04 feeders exhibit evident urban occupation but lack electrical infrastructure coverage in the official data. This absence, combined with the high percentage of commercial losses recorded in these feeders, suggests that these areas may correspond to irregular settlements or illegal connections.

Furthermore, the spatial detail provided by the segmentation of Google Earth images enabled a more precise identification of urban occupation areas, while the Landsat 8 images, with their lower resolution, posed challenges in detecting smaller clusters. Therefore, the combination of segmentation data with the

analysis of electrical infrastructure proved effective in identifying potentially problematic regions, providing valuable insights for better management and monitoring efforts.

5 CONCLUSIONS

The combination of CNNs with geospatial analysis techniques has proven effective in detecting irregular occupations in urban areas, integrating population, infrastructure, and satellite data. However, the study has limitations, such as geographic restrictions (Sabará, Minas Gerais), reliance on specific satellite data (Google Earth and Landsat 8), and the lack of real-time integration with utility operational systems.

Figure 7: Prediction results for the Google Earth satellite image dataset. (a) Ground truth; (b) LinkNetB7 BCEIoU; (c) LinkNetB7 DICE BCE; (d) D-LinkNet50 BCEIoU; (e) D-LinkNet50 DICE BCE.
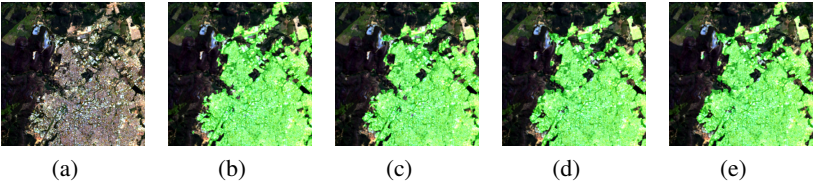

Figure 8: Prediction results overlaid on the original for the Landsat 8 satellite image dataset. (a) Original satellite image; (b) LinkNetB7 BCEIoU; (c) LinkNetB7 DICE BCE; (d) D-LinkNet50 BCEIoU; (e) D-LinkNet50 DICE BCE.

Figure 9: Prediction results for the Landsat 8 satellite image dataset. (a) Ground truth; (b) LinkNetB7 BCEIoU; (c) LinkNetB7 DICE BCE; (d) D-LinkNet50 BCEIoU; (e) D-LinkNet50 DICE BCE.
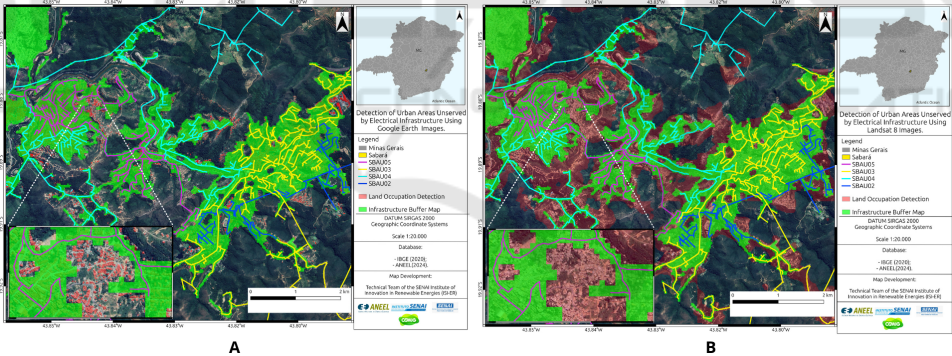

Figure 10: Land Use Prediction Using (A) Google Earth Satellite Images , (B) Landsat 8 Satellite and CEMIG Electrical Grid Coverage.

To advance, future research should expand the geographic scope, incorporate real-time and diverse data (socioeconomic and urban expansion), and explore more advanced neural architectures or hybrid models. Additionally, the development of a decision-support framework for utilities, with urban monitoring tools and demand forecasting, can enhance energy planning. Studies on the socioeconomic impacts of irregular settlements are also necessary for more comprehensive policies.

This research paves the way for artificial intelligence applications in urban energy management, promoting sustainable development and equitable resource distribution.

ACKNOWLEDGEMENTS

REFERENCES

Abujayyab, S. K., Almajalid, R., Wazirali, R., Ahmad, R., Taşoğlu, E., Karas, I. R., and Hijazi, I. (2023). Integrating object-based and pixel-based segmentation for building footprint extraction from satellite images. *Journal of King Saud University-Computer and Information Sciences*, 35(10):101802.

Afaq, S. and Rao, S. (2020). Significance of epochs on training a neural network. *Int. J. Sci. Technol. Res*, 9(06):485–488.

Akyel, C. and Arıcı, N. (2022). Linknet-b7: noise removal and lesion segmentation in images of skin cancer. *Mathematics*, 10(5):736.

ANEEL (2025). Energy loss reports - light in the tariff. Accessed: January 3, 2025.

Archana, R. and Jeevaraj, P. E. (2024). Deep learning models for digital image processing: a review. *Artificial Intelligence Review*, 57(1):11.

Ataş, İ. (2023). Performance evaluation of jaccard-dice coefficient on building segmentation from high resolution satellite images. *Balkan Journal of Electrical and Computer Engineering*, 11(1):100–106.

Avdan, U. and Jovanovska, G. (2016). Algorithm for automated mapping of land surface temperature using landsat 8 satellite data. *Journal of sensors*, 2016(1):1480307.

Batchkala, G. and Ali, S. (2021). Real-time polyp segmentation using u-net with iou loss.

Chaurasia, A. and Culurciello, E. (2017). Linknet: Exploiting encoder representations for efficient semantic segmentation. In *2017 IEEE visual communications and image processing (VCIP)*, pages 1–4. IEEE.

EPE (2024). Balanço Energético Nacional 2024. Acesso em: 30 set. 2024.

Flores, J. L. O. et al. (2023). Consumo de energia e crescimento econômico no brasil.

Gonzalez, R. C. and Woods, R. E. (2000). *Processamento de imagens digitais*. Editora Blucher.

Gorelick, N. (2013). Google earth engine. In *EGU general assembly conference abstracts*, volume 15, page 11997. American Geophysical Union Vienna, Austria.

He, Z., Yao, W., Shao, J., and Wang, P. (2024). Ub-finenet: Urban building fine-grained classification network for open-access satellite images. *ISPRS Journal of Photogrammetry and Remote Sensing*, 217:76–90.

Jiwani, A., Ganguly, S., Ding, C., Zhou, N., and Chan, D. M. (2021). A semantic segmentation network for urban-scale building footprint extraction using rgb satellite imagery. *arXiv preprint arXiv:2104.01263*.

Khan, A. and Sudheer, M. (2022). Machine learning-based monitoring and modeling for spatio-temporal urban growth of islamabad. *The Egyptian Journal of Remote Sensing and Space Science*, 25(2):541–550.

Li, S. and Liu, X. (2022). Multi-type road extraction and analysis of high-resolution images with d-linknet50. In *2022 3rd International Conference on Geology, Mapping and Remote Sensing (ICGMRS)*, pages 244–248. IEEE.

Montazerolghaem, M., Sun, Y., Sasso, G., and Haworth, A. (2023). U-net architecture for prostate segmentation: the impact of loss function on system performance. *Bioengineering*, 10(4):412.

Rani, K. P., Rao, K. S., Sreedevi, P., Subbaraju, G. V., Dastagiriah, C., and Padmavathi, J. (2024). Land cover extraction from satellite imagery using u-net model. In *Proceedings of the 11th International Conference on Computing for Sustainable Global Development*, pages 1361–1367.

Rosa, M., Shimbo, J. Z., and Azevedo, T. (2019). Mapbiomas-mapeando as transformações do território brasileiro nas últimas três décadas. *VIII Simpósio de Restauração Ecológica*, pages 95–100.

Sirko, W., Kashubin, S., Ritter, M., Annkah, A., Bouchareb, Y. S. E., Dauphin, Y., Keysers, D., Neumann, M., Cisse, M., and Quinn, J. (2021). Continental-scale building detection from high resolution satellite imagery. *arXiv preprint arXiv:2107.12283*.

Solomon, C. and Breckon, T. (2013). *Fundamentos de processamento digital de imagens-Uma abordagem prática com exemplos em MatLab*.

Ullah, S., Qiao, X., and Abbas, M. (2024). Addressing the impact of land use land cover changes on land surface temperature using machine learning algorithms. *Scientific Reports*, 14(1):18746.

Zhou, L., Zhang, C., and Wu, M. (2018). D-linknet: Linknet with pretrained encoder and dilated convolution for high resolution satellite imagery road extraction. In *Proceedings of the IEEE conference on computer vision and pattern recognition workshops*, pages 182–186.

Ágton de Oliveira, P. (2020). Deep learning na segmentação automática de imagens de satélite. 24 pages. Trabalho de Conclusão de Curso (Graduação) - Engenharia Agrícola e Ambiental.